

A Robust site-specific Au@SiO₂@AgPt nanorod/nanodots
superstructure for in-situ SERS monitoring catalytic reaction

Hao Wei Jia,^{a,b†} Li Qiu,^{a,b†} Jin Wang^{b*}

^a College of Materials Science and Engineering, University of Science and Technology of China,
Anhui 230026, P. R. China

^b Institute of Intelligent Machines, Chinese Academy of Sciences, Hefei, Anhui 230031, P. R.
China

* *Corresponding author. Email address: jwang@iim.ac.cn or wangjin_hf@yahoo.com*

†These authors contributed equally to this work.

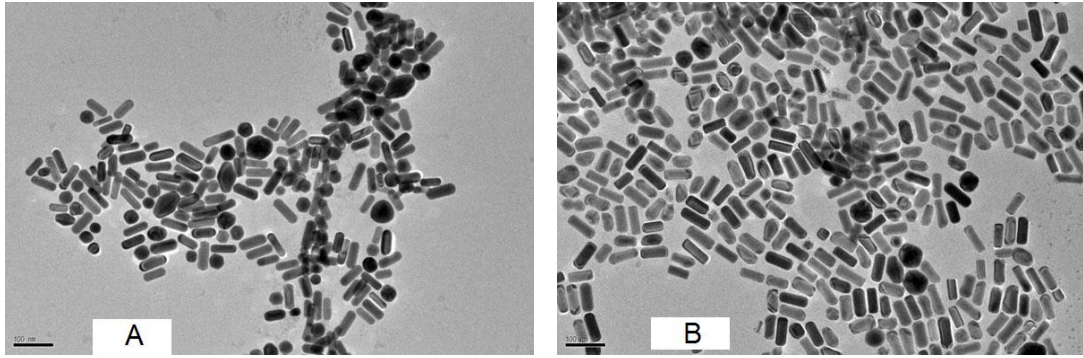


Fig. S1 TEM of Au@SiO₂ nanorods (A); Au@SiO₂@Ag nanorods (B)

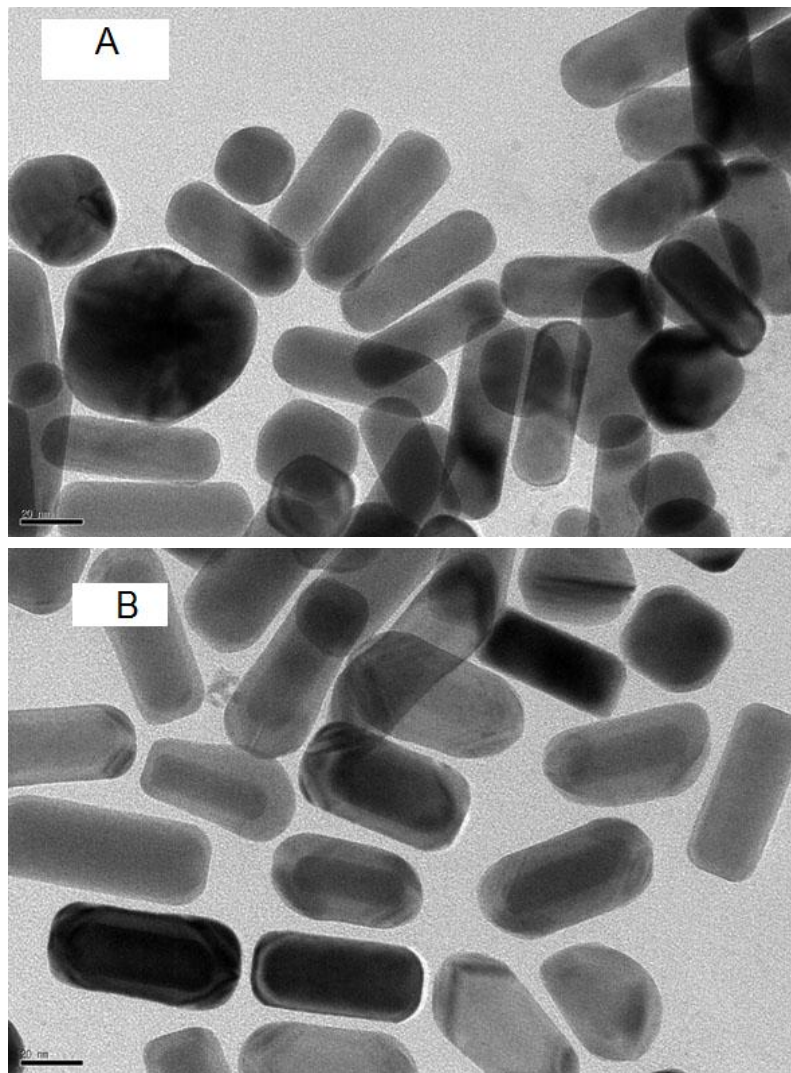


Fig. S2 Magnified image of TEM of Au@SiO₂ nanorods (A); Au@SiO₂@Ag nanorods (B)

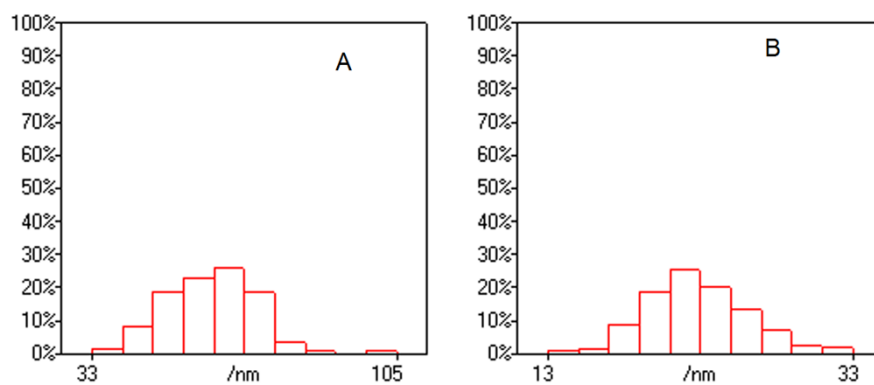


Fig. S3 (A) The histogram of edge length of Au@SiO₂ nanorods (corresponding to Fig. S1A), the average edge length is 61.15 ± 10.46 nm. (B) The histogram of width of Au@SiO₂ nanorods (corresponding to Fig. S1A), the average width is 22.87 ± 3.34 nm

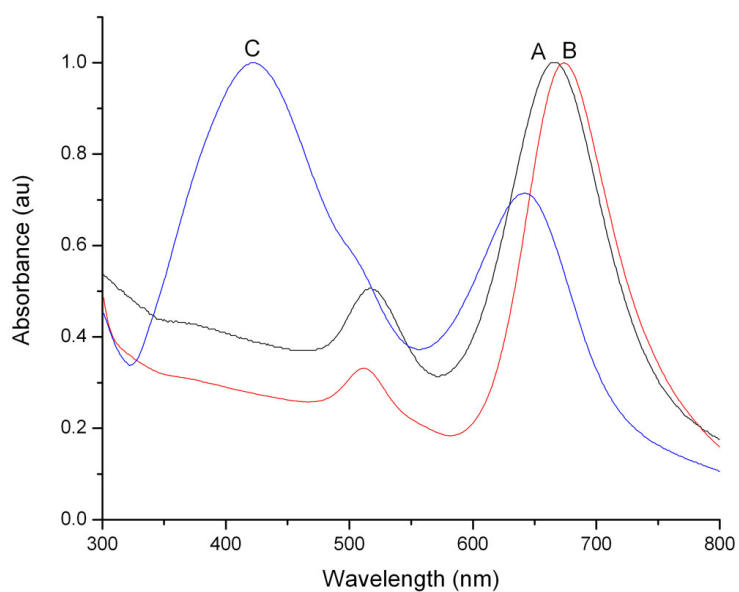


Fig. S4 UV-vis-NIR spectrum of Au nanorods (A); Au@SiO₂ nanorods (B); Au@SiO₂@Ag nanorods (C)

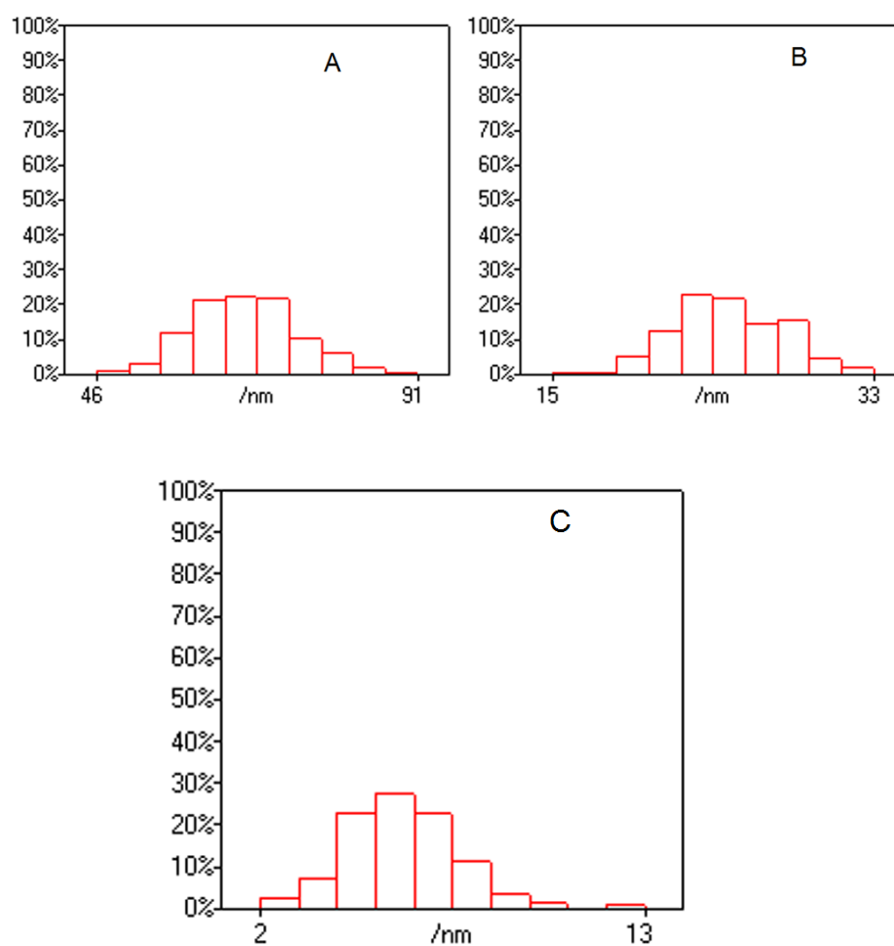


Fig. S5 (A) The histogram of edge length of Au@SiO₂@Ag nanorods (corresponding to Figure S1B), the average edge length is 66.78 ± 7.29 nm. (B) The histogram of width of Au@SiO₂@Ag nanorods (corresponding to Figure S1B), the average width is 24.93 ± 3.01 nm. (C) The histogram of thickness of Au@SiO₂@Ag nanorods (corresponding to Figure S1B), the average thickness of 6.08 ± 1.62 nm.

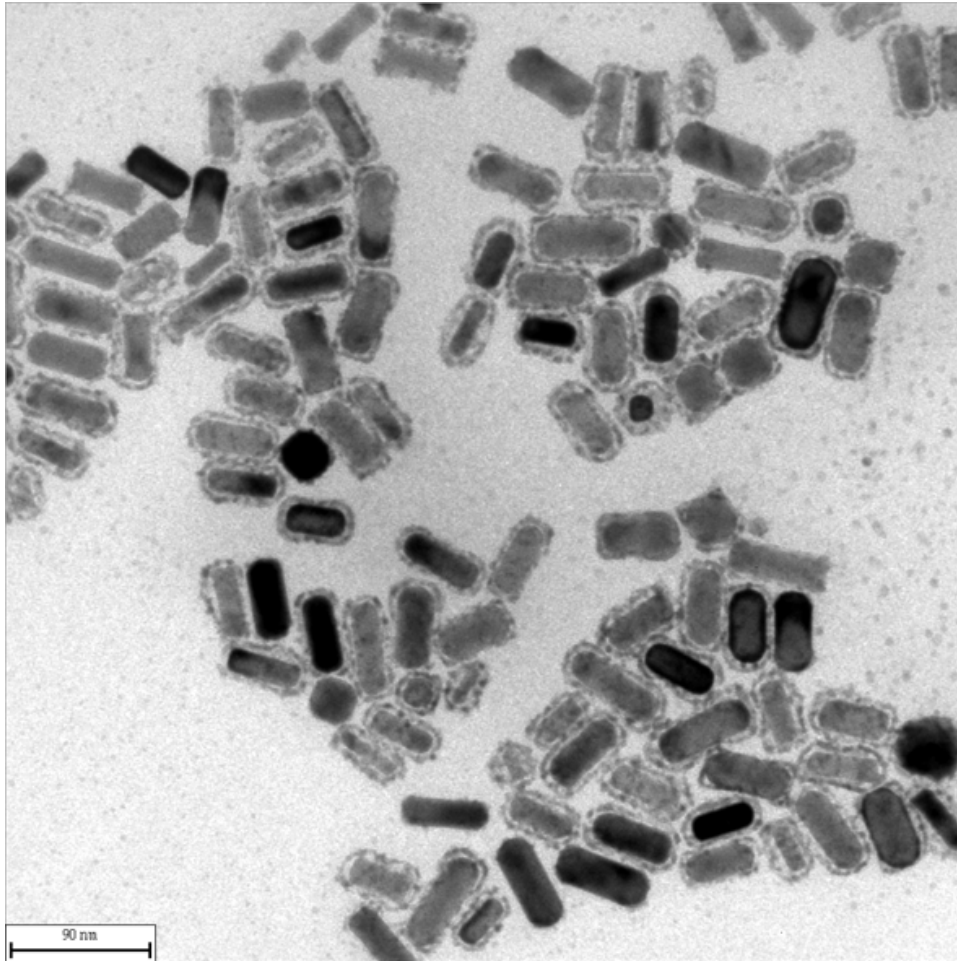
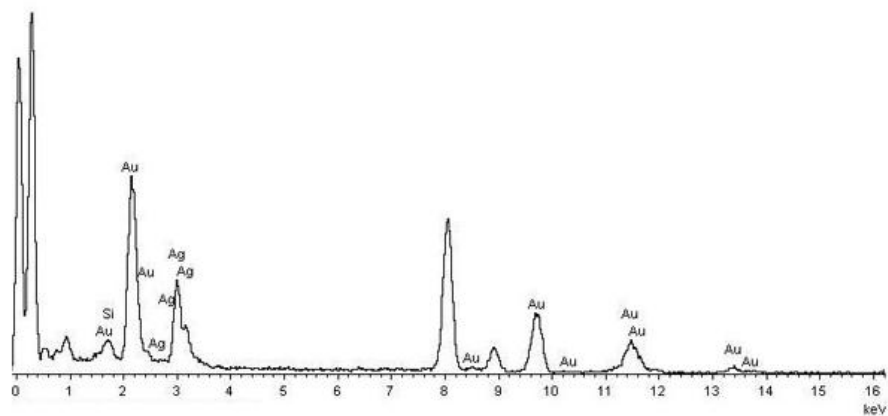
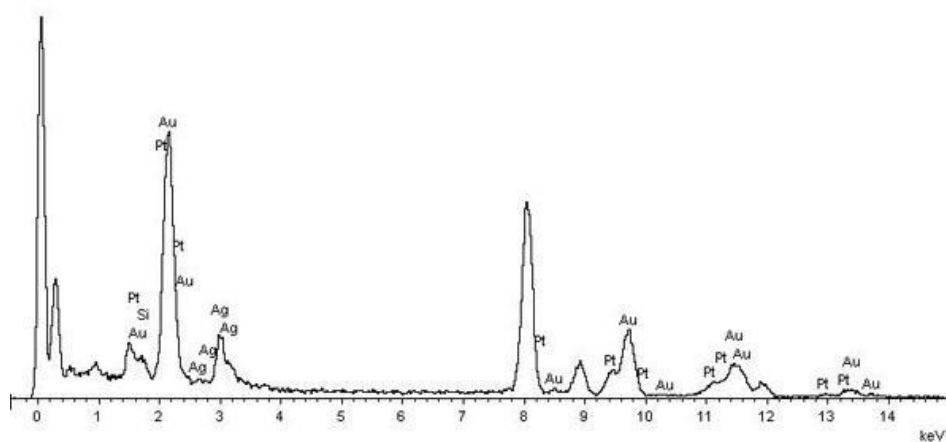


Fig. S6 Low magnification and large field view of the TEM images of tip-edge coated Au@SiO₂@AgPt nanorod/nanodots superstructure.



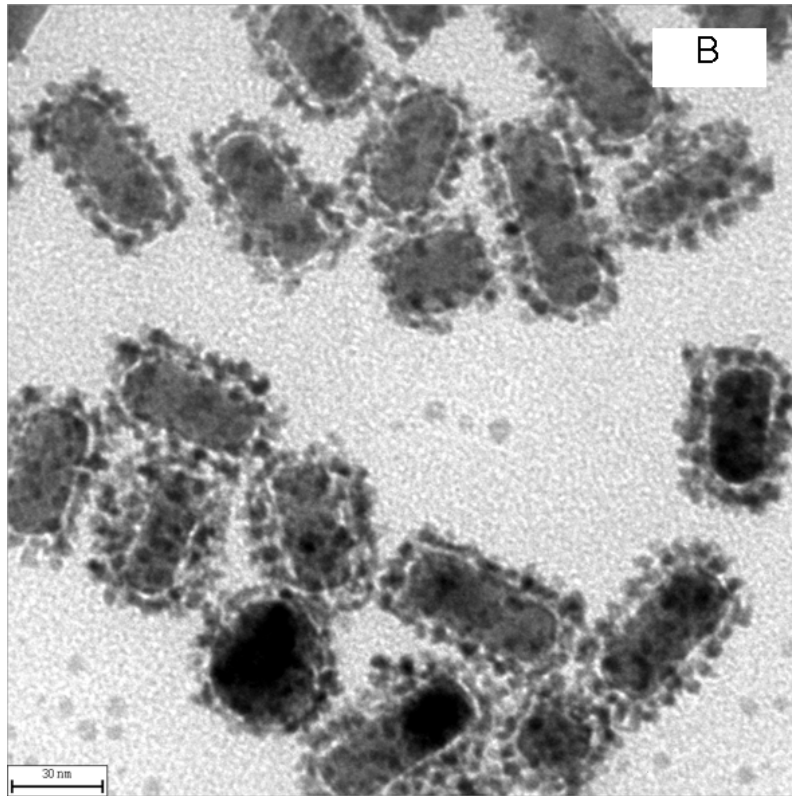
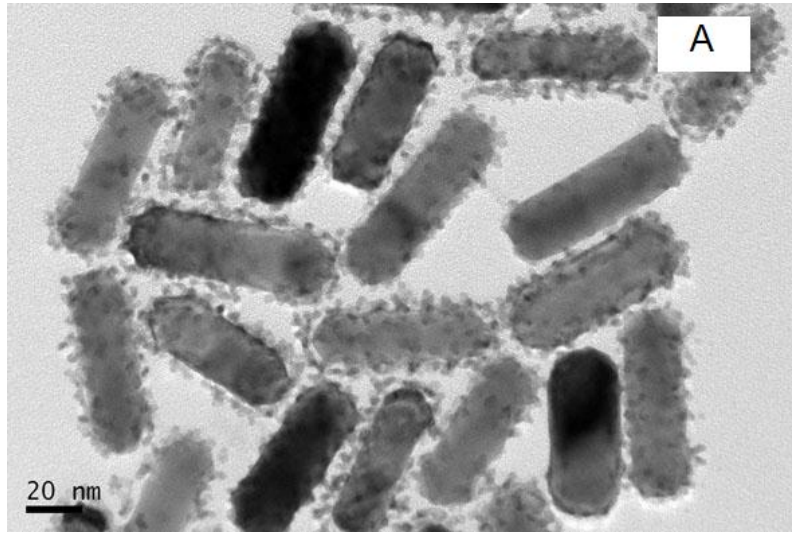
Element	Peak	Area	k	Abs	Weight%	Weight%	Atomic%
	Area	Sigma	factor	Corn.		Sigma	
Si K	606	110	0.732	1.150	1.66	0.30	8.31
Ag L	7943	306	1.262	1.127	36.86	1.04	47.92
Au M	14499	335	1.194	1.089	61.48	1.05	43.78
Totals					100.00		

Fig. S7 The EDX percentage of Au@SiO₂@Ag core-shell nanorods



Element	Peak	Area	k	Abs	Weight%	Weight%	Atomic%
	Area	Sigma	factor	Corn.		Sigma	
Si K	620	121	0.732	1.143	1.65	0.32	9.16
Ag L	4242	261	1.262	1.154	19.63	1.07	28.39
Pt M	3779	362	1.190	1.095	15.65	1.30	12.51
Au M	15186	393	1.194	1.095	63.06	1.37	49.94
Totals					100.00		

Fig. S8 The EDX percentage of core-satellite Au@SiO₂@AgPt nanorod/nanodots superstructure



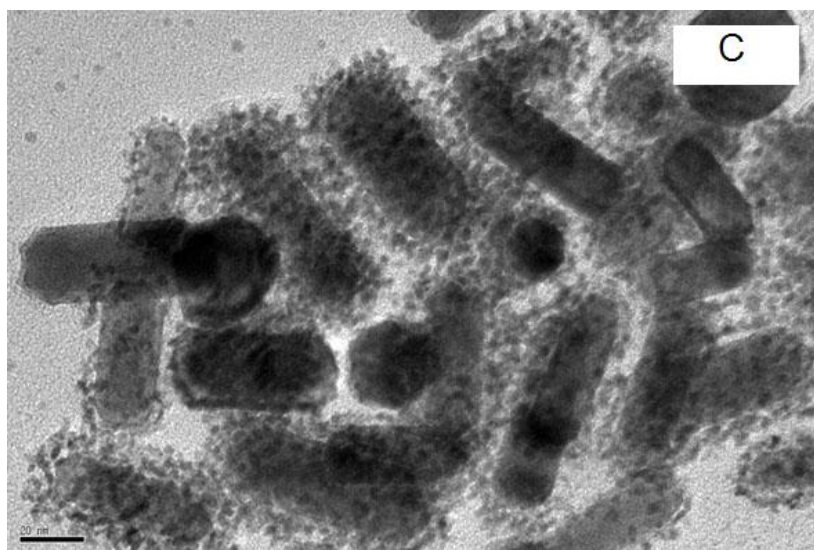


Fig. S9 TEM of Au@SiO₂@AgPt nanorods/nanodots superstructure with different amounts of AgNO₃ (A) 0.5 mL 4mM; (B) 1 mL 4mM; (C) 1.5 mL 4mM and identical 38.6 mM H₂PtCl₆ 1 mL.

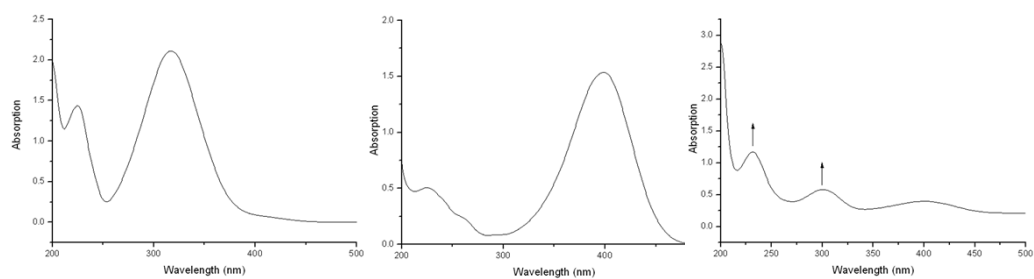
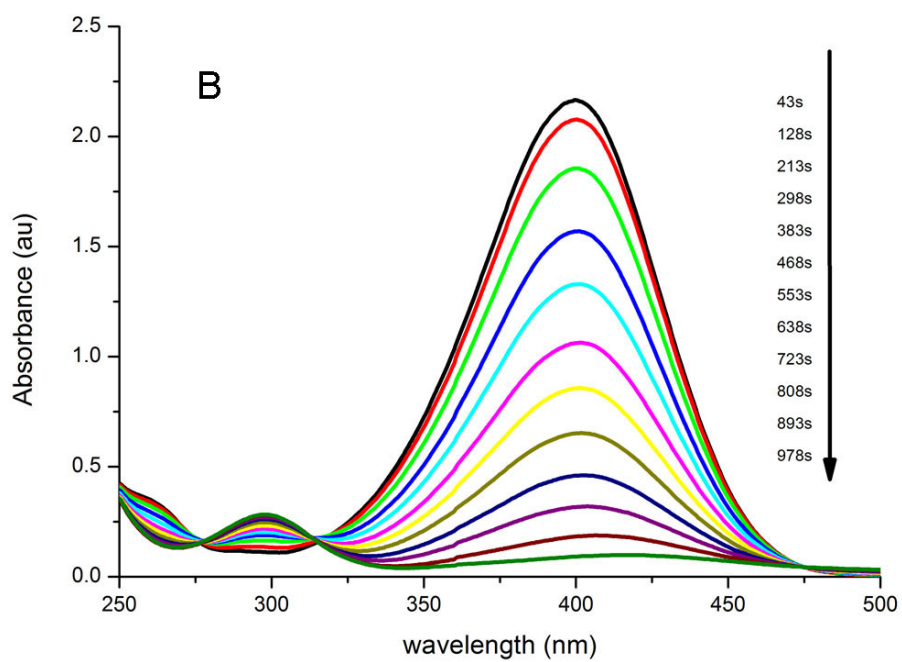
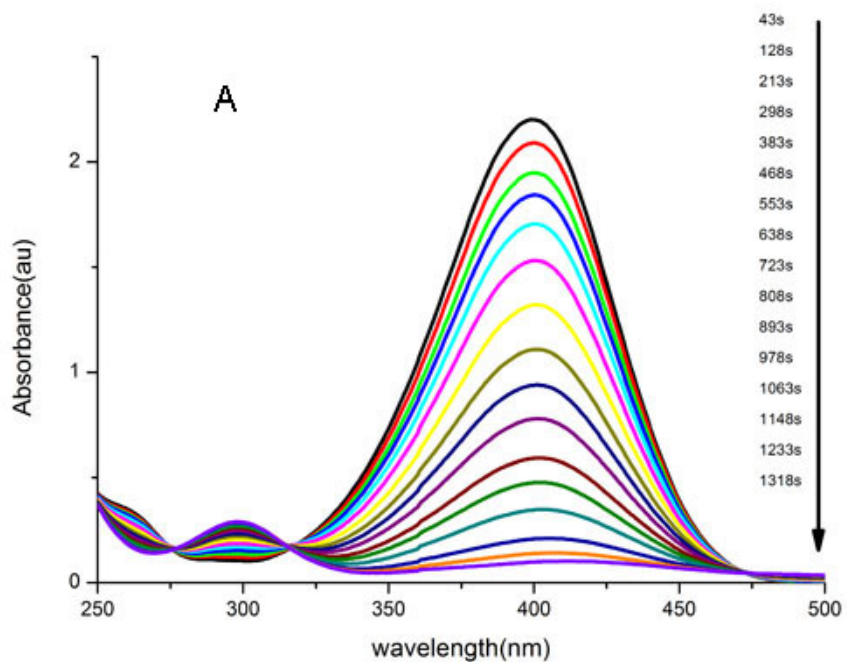
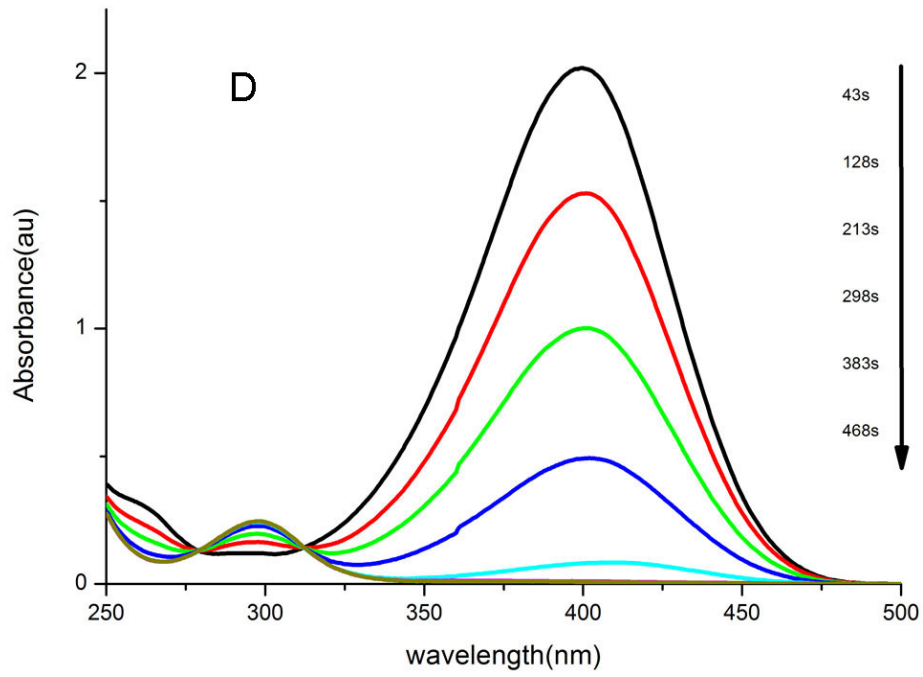
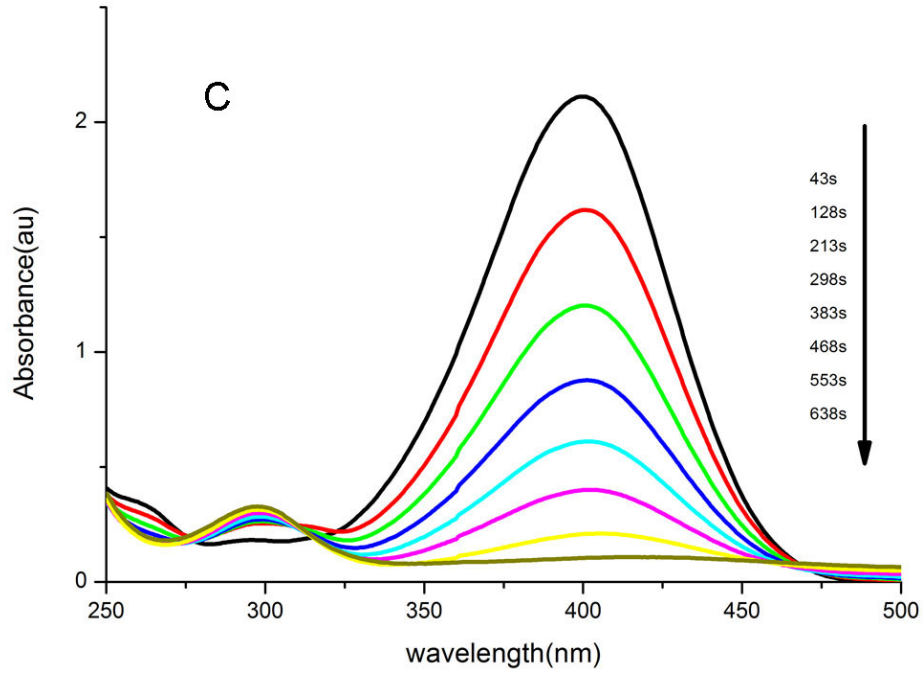


Fig. S10 UV-Vis spectrum of 4-nitrophenol (left); UV-Vis spectrum of p-nitrophenolate anions when NaBH₄ is added to 4-nitrophenol (middle); UV-Vis spectrum of p-aminophenolate anions when nanorods/nanodots are added to the mixture of NaBH₄ and p-nitrophenol (right)





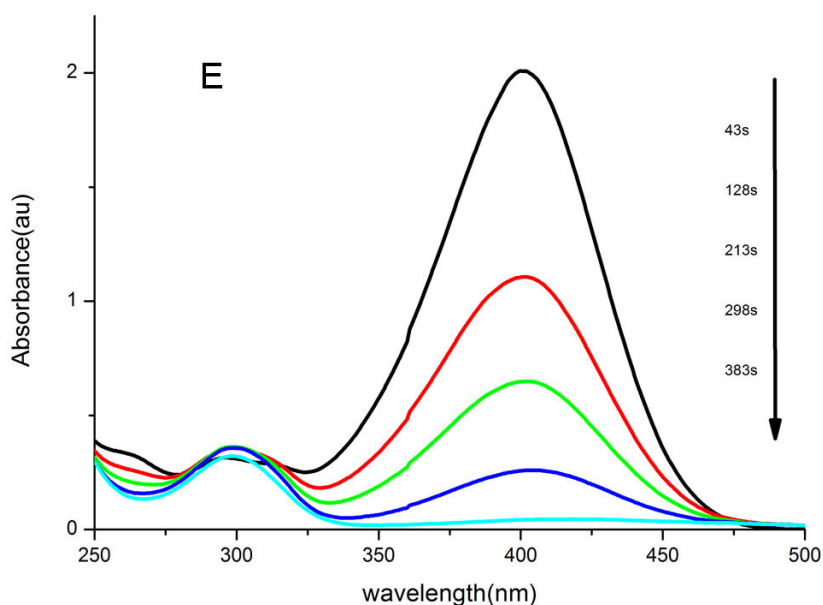


Fig. S11 The successive decrease of the UV-Vis spectrum of the reduction of p-nitrophenol by using (A) Au@SiO₂@Ag nanorods; (B) tip coated Au@SiO₂@AgPt nanorod/nanodots superstructure; (C) tip/edge coated Au@SiO₂@AgPt nanorod/nanodots superstructure; (D) core-satellite Au@SiO₂@AgPt nanorod/nanodots with low Pt density superstructure; (E) core-satellite Au@SiO₂@AgPt nanorod/nanodots with high Pt density superstructure

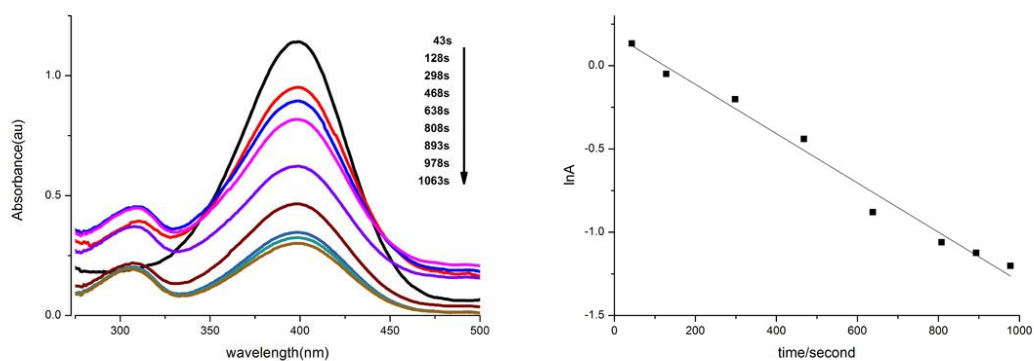


Fig. S12 The successive decrease of the UV-vis spectrum of the reduction of p-nitrophenol by Pt nanodots (left); Plots of lnA versus time for the reduction of para-nitrophenol catalysis by Pt nanodots.

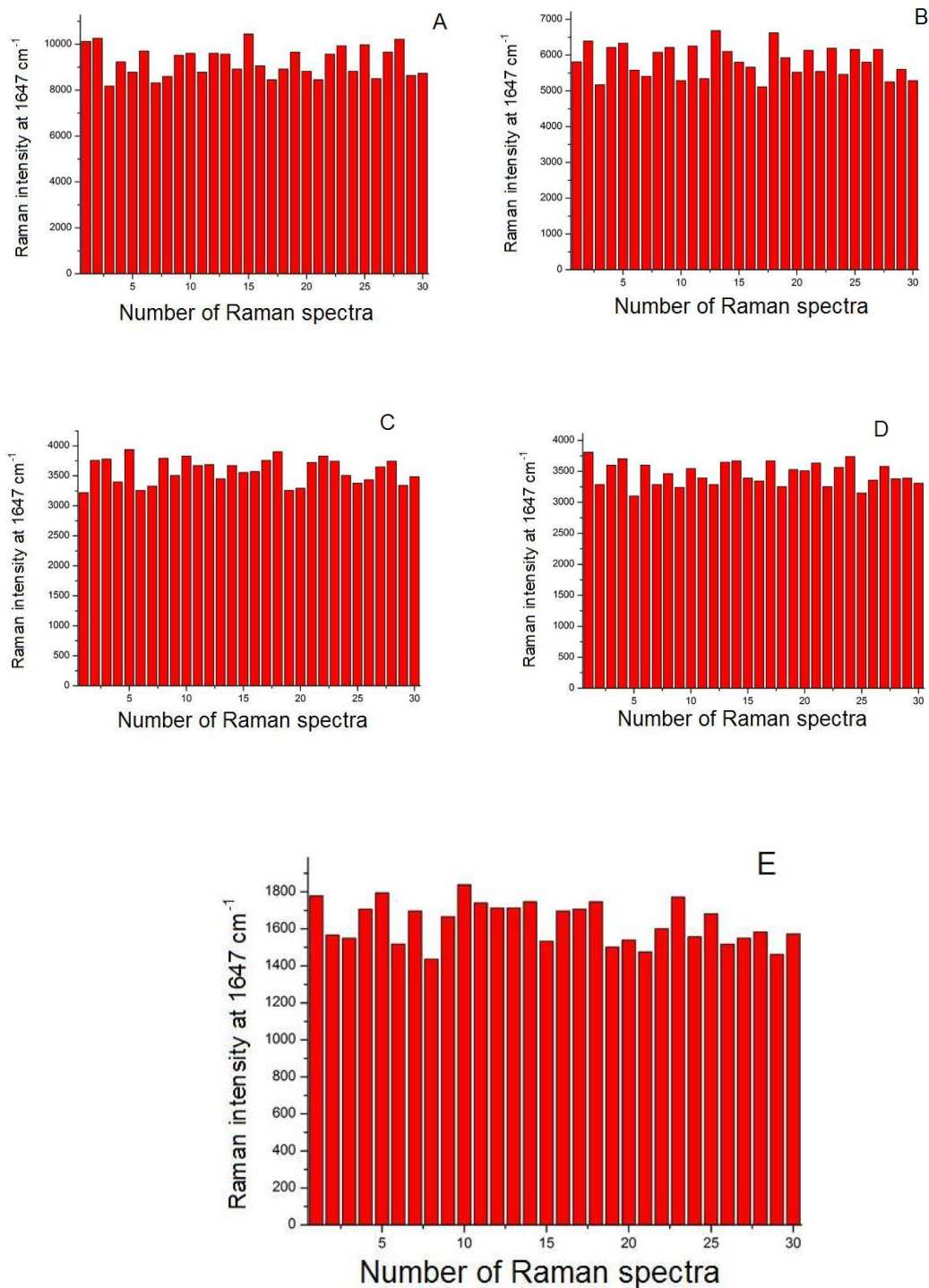


Fig. S13 The intensity of the main Raman vibrational of R6G with concentration 10^{-7} M in 30 points SERS spectra collected on the (A) Au@SiO₂@Ag core-shell nanorods, (B) tip coated Au@SiO₂@AgPt nanorod/nanodots superstructure; (C) tip/edge coated Au@SiO₂@AgPt nanorod/nanodots superstructure; (D) core-satellite Au@SiO₂@AgPt nanorod/nanodots with low Pt density superstructure; (E) core-satellite Au@SiO₂@AgPt nanorod/nanodots with high Pt density superstructure